Reliability Assessment of Distribution Systems Under Influence of Stochastic Nature of PV and Spatial-temporal Distribution of EV Load Demand

Lei Xiao, *Student Member*, *IEEE*, Kashem M. Muttaqi, *Fellow*, *IEEE*, and Ashish P. Agalgaonkar, *Senior Member*, *IEEE*

***Abstract*—With the progressive exhaustion of fossil energy and growing concerns about climate change, it has been observed that distributed energy resources such as photovoltaic (PV) systems and electric vehicles (EVs) are being increasingly integrated into distribution systems. This underscores the increasing imperative for a thorough analysis to evaluate reliability from the perspectives of distribution systems and EV charging services, taking into account the stochastic nature of PV and EV load demands. This paper presents an approach for the reliability assessment of distribution systems that incorporate PV and EVs considering reliability models for both PV systems and EV battery systems. It also defines new indices to investigate the adequacy and customer-side reliability for EV charging services. The developed methodology utilizes a Monte Carlo simulation-based approach and is showcased using the modified Roy Billinton Test System (RBTS) Bus 4 distribution system. The results illustrate that reliability indices for EV charging services, such as percentage of charging energy not supplied (PCENS), average EV interruption frequency index (AEVIFI) and average EV interruption duration index (AEVIDI), are improved under the proposed approach.**

***Index Terms*—Distribution system, reliability, charging, electric vehicle (EV), interruption frequency, interruption duration, load demand.**

I. Introduction

ELECTRIC vehicles (EVs) are becoming popular due to their declining costs and zero emission. As EV penetration increases, the transportation and distribution systems are becoming highly interactive [1]. However, the rapid expansion of EV load demand poses challenges to the existing power grid as EVs consume significant amounts of electrical energy which can result in unwanted peaks in electricity consumption [2], [3]. The variability of spatial-temporal EV load demands and photovoltaic (PV) generation complicates the integration of large amounts of distributed energy resources into the grid and presents challenges for reliability assessment. Meteorological conditions, particularly cloud movements, are responsible for the notable uncertainties in PV power output, resulting in highly variable solar irradiance [4]. For EVs, the diversity in charging characteristics, such as the number of charging EVs, battery capacity and status, and charging duration, adds to the uncertainty in the distribution system [5].

Over the past few years, numerous studies have concentrated on the reliability assessment of distribution systems incorporating distributed energy resources and EVs. Table I provides a comparison of techniques, resources integrated into the distribution system, and reliability indices utilized in literature. As depicted in Table I, researchers commonly employ well-established indices to assess the reliability of distribution systems, such as loss of load probability (LOLP), system average interruption frequency index (SAIFI), system average interruption duration index (SAIDI), expected energy not served (EENS), energy not supplied (ENS), average energy not supplied (AENS), loss of load expectation (LOLE), customer average interruption duration index (CAIDI), average service unavailability index (ASUI), and average service availability index (ASAI). In [6], a reliability evaluation of the distribution network considering the integration of PV, wind turbine generators (WTGs), and energy storage systems (ESSs) is presented, incorporating the stochastic characteristics of the primary components of renewable resources. The reliability of customers within a microgrid featuring distributed generation (DG) is assessed in [7]. In [8], an integrated Markov model is suggested to assess the DG reliability of future distribution networks. The reliability of distribution systems with DGs is evaluated in [9]. In [10] and [11], analytical techniques are recommended to analyze the reliability of distribution systems that include DGs. Reference [12] investigates distribution system reliability considering the impact of an EV battery swapping station. In [13], the influence of integrated renewable and distributed energy resources is considered in the distribution system reliability assessment. A new approach is developed to study the effect of EVs using the battery exchange mode on the power system reliability in [14], and a new index named user demand not satisfied

Manuscript received: March 28, 2024; revised: June 5, 2024; accepted: October 8, 2024. Date of CrossCheck: October 8, 2024. Date of online publication: October 24, 2024.

This article is distributed under the terms of the Creative Commons Attribution 4.0 International License (http://creativecommons.org/licenses/by/4.0/).

L. Xiao (corresponding author), K. M. Muttaqi, and A. P. Agalgaonkar are with the Australian Power and Energy Research Institute (APERI), School of Electrical, Computer and Telecommunications Engineering, University of Wollongong, Wollongong, NSW 2522, Australia (e-mail: lx626@uowmail. edu. au; kashem@uow.edu.au; ashish@uow.edu.au).

DOI: 10.35833/MPCE.2024.000336

(UDNS) is introduced. Reference [15] investigates the reliability of active distribution networks with DGs, taking into account customer satisfaction. Additionally, four indices, namely voluntary interruption frequency (VIF), voluntary adjustment frequency (VAF), annual purchased electricity (E_{purchase}) and probability to purchase electricity (P_{purchase}) are proposed for evaluating the impacts of customer satisfaction on the reliability. In [16], a Monte Carlo simulation (MCS) algorithm is applied to evaluate the reliability of a modified RBTS Bus 6 distribution system that includes conventional and renewable DGs. Reference [17] uses an analytical approach to study the prospective function of EV charging stations in improving the distribution system reliability. The impacts of parking lots on modern distribution system reliability are assessed in [18]. In [19], the influences of significant EV integration on both system reliability and EV charging service reliability are discussed. While new indices like charging energy not supplied (CENS) and percentage of curtailed charging energy (POCCE) are introduced, the primary emphasis lies on assessing charging adequacy rather than the reliability of EV-owner-side charging services. Reference [20] presents a MCS method for computing the reliability of the distribution system incorporating DGs. A new algorithm for evaluating the reliability of active distribution systems with microgrids is proposed in [21]. MCS is a commonly employed technique for evaluating the reliability of distribution systems incorporating renewable energy resources [22], [23]. It has the advantage of being able to simulate almost any system and failure mode, but it necessitates a large number of samples, and its precision could be affected by the quantity of runs and variables within the system.

TABLE I
COMPARISONS OF LITERATURE FOR RELIABILITY ASSESSMENT OF DISTRIBUTION SYSTEM

Reference	Technique	Resource	Main reliability index
[6]	Analytical	WTG, ESS, PV	SAIFI, SAIDI, CAIDI, AENS, EENS
[7]	Analytical	PV, diesel generator	SAIFI, SAIDI, EENS
[8]	Analytical	PV, WTG, conventional DG (diesel, gas)	LOLP, SAIFI, SAIDI
[9]	MCS	PV, WTG, geothermal, waste to energy	ENS
[10]	Analytical	WTG, PV, micro-turbine generator, ESS	SAIFI, SAIDI, ENS
[11]	Analytical	Conventional and renewable DGs	SAIFI, SAIDI
[12]	MCS	EVs	SAIFI, SAIDI, EENS
[13]	MCS	PV, battery ESS, EVs	SAIFI, SAIDI, CAIDI
[14]	MCS	EVs	EENS, UDNS
[15]	MCS	PV, WTG, ESS	SAIFI, EENS, VIF, VAF, E_{purchase}, P_{purchase}
[16]	MCS	Conventional and renewable DGs	SAIFI, SAIDI
[17]	Analytical	EVs	SAIFI, SAIDI, EENS
[18]	MCS	EVs, PV, diesel generator, WTG, micro-turbine	AENS, SAIDI
[19]	MCS	EVs, PV	SAIFI, SAIDI, EENS, CENS, POCCE
[20]	MCS	DGs	SAIFI, SAIDI, CAIDI
[21]	MCS	WTG, PV, gas turbine	SAIFI, EENS, ASUI

While numerous previous studies have explored distribution system reliability, these studies often neglect to include PV system and EV battery system fault rates in their assessments. Additionally, the existing literature primarily focuses on distribution system reliability rather than taking into account the perspective of EV owners. However, with the increasing penetration of EVs in distribution systems, there is a growing need for a more thorough analysis that incorporates factors such as EV load demands and evaluates reliability from the perspective of EV charging services. In [24], an approach is developed to examine the reliability of charging services and the corresponding costs of PV-powered charging stations situated along a highway. Nevertheless, the emphasis is placed on the charging stations rather than the distribution system. Recognizing these research gaps, this paper aims to investigate the impacts of EV load demands and PV output on both the distribution system reliability and the EV charging service reliability.

This paper proposes an MCS-based approach for investigating the adequacy and customer-side reliability indices. The primary contributions of this paper can be outlined as follows.

1) An MCS-based approach is developed to investigate the stochastic characteristics related to uncertain PV output, EV load demands, and the subsequent reliability implications. The impacts of the spatial-temporal distribution of EV load demands and PV output on the adequacy and customer-side reliability indices are measured.

2) A PV multistate model is applied to the estimation of PV generation considering the failure rate associated with each individual PV unit integrated within the PV system. This approach facilitates more accurate PV generation predictions, thereby assessing the adequacy of a PV system accurately.

3) A travel chain is utilized to delineate the travel patterns of EV users across three functional areas during weekdays. The assessment of EV load demands encompasses the reliability of EV battery systems and the employed EV charging

strategies.

4) New indices are defined to assess the EV charging service reliability, such as PCENS, AEVIFI, and AEVIDI. PCENS is proposed as an index for EV charging adequacy assessment, while AEVIFI and AEVIDI are defined to study EV-owner-side reliability.

5) Extensive case studies are provided to evaluate the associated reliability indices for different scenarios to showcase the impacts of different capacity levels of the PV system and travel distances of EVs under different charging strategies on the reliability of the distribution system for different areas, and the effects of altering area distributions on EV charging service reliability indices.

The computational studies in this paper utilize a modified Roy Billinton Test System (RBTS) Bus 4 distribution system with the integration of PV systems and EVs. The indices used in the paper are for both the distribution system and EV charging services, as illustrated in Table II. The LOLP index is used to study the PV islanded distribution system adequacy, while SAIFI and SAIDI are calculated to assess customer-side reliability for different areas in the distribution system.

TABLE II
RELIABILITY INDICES

Type	Adequacy assessment index	Customer-side reliability index
Distribution system	LOLP	SAIFI, SAIDI
EV charging service	PCENS	AEVIFI, AEVIDI

The subsequent sections of the paper are structured as follows. Section II delineates a model of a PV system for reliability investigations considering the impact of cloud and PV subsystem reliability. Section III introduces the stochastic model of travel behavior, the reliability model of EV battery systems, and the EV charging strategy for the evaluation of the impact of spatial-temporal distribution of EV load demands on the reliability of distribution systems and EV charging services. In Section IV, simulation results illustrating the application of the proposed approach to a test system are depicted. Concluding remarks are provided in Section V.

II. MODELING PV FOR RELIABILITY STUDIES

In this study, a PV system employed in solar farms is embedded in the distribution system. This section establishes a framework for the PV system model. The electrical output generated by a PV system is estimated considering both the impact of cloud and the hourly operating history of the PV subsystem. In addition, indices for assessing the reliability of the PV islanded system are introduced in this section.

A. PV Output Model

The purpose of a PV system is to produce electrical energy by transforming sunlight into usable power. The amount of solar radiation received is the primary factor that determines the generated power from the PV system. Cloudiness is a significant factor impacting the variance in solar radiation values recorded beyond the atmosphere, which are nearly constant, and the radiation measured on the Earth's surface. A clearness index k_t is employed to adjust for the influence of clouds, and its probability density function $f(k_t)$ can be expressed using (1), as depicted in Fig. 1.

$$f(k_t)=\frac{C(k_{tu}-\overline{k_t})}{k_{tu}}\mathrm{e}^{\lambda k_t} \tag{1}$$

where k_{tu} is the upper bound for k_t, and k_{tu} is considered constant at the value of 0.864 in this model; $\overline{k_t}$ is the mean hourly clearness index from historical data; and C and λ are the functions of k_{tu} and $\overline{k_t}$, respectively [25].

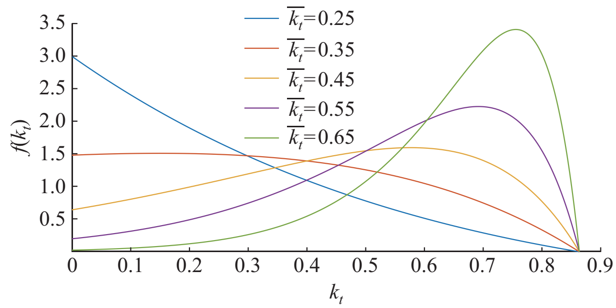

Fig. 1. Plot of proposed probability density function.

The power output of a PV system P_{pv} can be predicted using the available solar radiation, as demonstrated in (2) [26].

$$P_{pv}=P_{rated}\frac{k_t H_0}{G_{stc}} \tag{2}$$

where P_{rated} is the rated capacity of the PV array under standard test conditions; H_0 is the solar irradiance from outside the Earth's atmosphere; and G_{stc} is the global horizontal radiation under standard test conditions.

B. PV Multistate Model

Grid-connected PV farms consist primarily of solar panels and inverters, which can be configured into either a central inverter structure or a string inverter structure. The difference between the two structures is that in the string inverter structure, each string is equipped with its own inverter to convert the DC electricity to AC outputs [27], [28].

In this paper, PV systems have solar panels and inverters as their primary components, which are interconnected in a string inverter configuration and can only operate when both the solar panels and the inverter are functional. Each string is treated as a subsystem to model the PV system. The solar panels and the inverter are represented as units with two states with corresponding failure rates and repair rates. These parameters enable the determination of the overall failure rate λ_{sub} and repair rate μ_{sub} of the subsystem. The PV multistate model is employed to estimate PV generation in the case study, taking into account the fault rate of each PV unit within the PV system.

It is assumed that the operating and repair state duration distribution functions for a two-state subsystem are exponential. The time to failure (TTF) and time to repair (TTR) are given as [22]:

$$TTF = -\frac{1}{\lambda_{sub}}\ln R \tag{3}$$

$$TTR = -\frac{1}{\mu_{sub}}\ln R' \tag{4}$$

where R and R' are the uniformly distributed random number sequences between [0, 1].

The state duration sampling method is used to simulate the chronological system state transition process, with further details in [22]. The approach involves constructing the chronological PV system state transition process by aggregating all chronological PV subsystem state transition processes. Consequently, the hourly output of a PV system $P_{pvsystem}(t)$ is the cumulative output generated by all PV subsystems, as depicted in (5).

$$P_{pvsystem}(t) = \sum_{i=1}^{n} P_{subsys,i}(t) S_{pv,i}(t) \tag{5}$$

where $P_{subsys,i}(t)$ is the hourly PV output of subsystem i at time t; and $S_{pv,i}(t)$ is the state of subsystem i. If subsystem i is not operating, $S_{pv,i}$ equals 0; otherwise, it equals 1.

C. Adequacy Assessment for a PV Islanded System

The role of PV systems is to enhance reliability by providing power to local loads during interruptions. The integration of PV into the distribution system can further enhance reliability by supplying loads during islanded operation. Assessing the adequacy of a PV islanded system typically involves convolving the dynamic output of the PV system with the load duration curve to determine the probability of meeting load demand. This analysis helps understand the effect of PV systems on system reliability during interruptions. In this study, it is assumed that in a PV islanded system, loads are supplied only by PV. The rated capacity ratio (RCR) [8] of a PV system is the ratio between the nameplate capacity of the PV and the annual load peak demand, as represented in (6).

$$RCR = \frac{P_{PVnc}}{L_{cust}} \tag{6}$$

where P_{PVnc} is the PV rated capacity; and L_{cust} is the annual customer load peak demand.

LOLP represents the probability that the available PV energy is lower than the load, serving as a metric to evaluate a PV islanded system adequacy. It can be computed by the ratio of total hours for which generation is less than demand to total number of hours, as shown in (7). A low LOLP value indicates a minimal probability of energy shortage compared to the load, signifying high system adequacy.

$$LOLP = \frac{\sum_{t=1}^{8760N_Y} D_t}{8760N_Y} \tag{7}$$

where N_Y is the cumulative number of simulation years; and D_t equals 1 if $P_{pvsystem}$ is less than the customer load demand and it equals 0 otherwise.

III. Impact of EVs on Reliability

In order to assess the spatial-temporal distribution of EV load demands, it is essential to evaluate each EV user's travel behavior, charging strategy, and operating history of EV battery systems. Travel chain is employed to delineate EV users' travel process among three functional areas on weekdays. EV load demands are evaluated taking into account the EV battery system reliability and charging strategy. Indices and evaluation procedure for both EV embedded distribution system reliability and EV charging service reliability are introduced.

A. Modeling Stochasticity with EV Travel Process

The basic characters utilized to depict each user's travel journey comprise the initial departure location, departure time, travel distance, driving speed, travel destination, and parking duration. These fundamental components constitute an EV travel chain that illustrates the journey of EVs. Specifically, the travel chain outlines the journey of an EV as it departs from one location at a predetermined time, proceeds to multiple destinations in defined sequence, and ultimately reaches its final destination [29]. The characters are described as follows.

1) Departure time

The probability of the first departure time for EVs is assumed to obey the normal distribution [29]. The probability density function of the first departure time $f(t_0)$ is given as:

$$f(t_0) = \frac{1}{\sigma_0\sqrt{2\pi}}\exp\left(-\frac{(t_0-\mu_0)^2}{2\sigma_0^2}\right) \tag{8}$$

where μ_0 is the average first departure time; t_0 is the first departure time; and σ_0 is the standard deviation of the first departure time.

2) Travel distance

The travel distance of each EV, denoted as l, satisfies a lognormal distribution [29], and its probability density function $f_l(l)$ is given as:

$$f_l(l) = \frac{1}{l\sigma_l\sqrt{2\pi}}\exp\left(-\frac{(\ln l-\mu_l)^2}{2\sigma_l^2}\right) \tag{9}$$

where μ_l is the average travel distance; and σ_l is the standard deviation of the travel distance.

3) Driving speed

The driving speeds of EVs are assumed to be uniformly distributed between 25 km/h and 45 km/h in secondary roads, and the unit kilometer energy consumption of EVs can be denoted as [29]:

$$c = 0.208 - 0.002v + 1.553/v \tag{10}$$

where v is the driving speed of an EV.

4) Initial departure location and travel destination

This study simulates the commuter's travel behavior in an urban area on weekdays. Based on the travel motive, the urban region is segmented into three functional areas: residential area, industrial area, and commercial area. The residential area pertains to the neighborhood where people reside; the industrial area comprises of office buildings, industrial buildings, and so on; and the commercial area encompasses large shopping malls, supermarkets, hotels, parks, and so on.

It is assumed that all EVs travel from the residential area for their first trip. In the first trip, the percentage of EV users going to the industrial area is ω, while the others going to the commercial area. The destinations for the second trip could be randomly chosen from the three areas, taking into account that certain individuals might have commitments such as work or other activities apart from returning home. The travel destination structure for EVs is shown in Fig. 2.

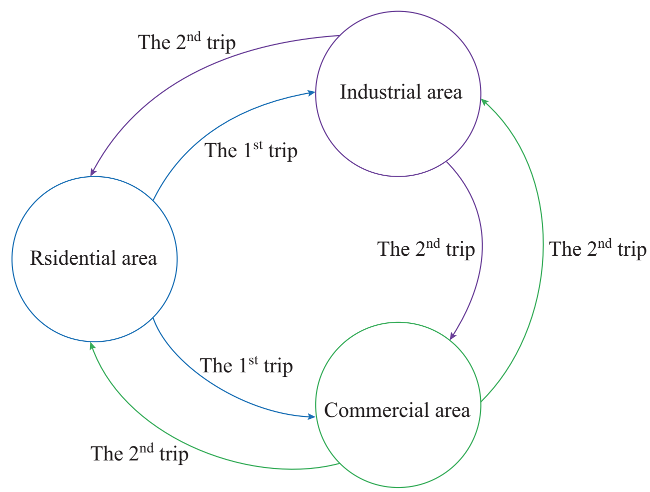

Fig. 2. Travel destination structure for EVs.

5) Parking duration

The duration an EV is parked at the destination restricts the time available for charging. In the first trip, the parking duration is assumed to follow a uniform distribution between 6 and 10 hours for the industrial area and is uniformly distributed between 4 and 6 hours for the commercial area. For the final destination, EVs will be parked until departure time for the next day.

B. Reliability Model for EV Battery Systems

In an EV battery system, the battery system connectors, battery management system (BMS) controllers, and battery modules are less reliable compared with other components [30]. Battery modules are energy storage components consisting of multiple battery cells, while BMS controllers are responsible for overseeing the battery system. They are integrated to function as one system, where any component failure can result in the failure of the entire EV battery system.

In order to evaluate the operational state of an EV battery system, the battery system connectors and battery modules as a whole and the BMS controllers are modeled as units with two states, characterized by failure rates (λ_{mod}, λ_{con}) and repair rates (μ_{mod}, μ_{con}), respectively.

The failure rate λ_{BEV} and repair rate μ_{BEV} for the EV battery system can be determined through (11) and (12), respectively.

$$\lambda_{BEV}=\lambda_{mod}+\lambda_{con} \tag{11}$$

$$\mu_{BEV}=\frac{\mu_{mod}\mu_{con}(\lambda_{mod}+\lambda_{con})}{\lambda_{mod}\mu_{con}+\lambda_{con}\mu_{mod}} \tag{12}$$

The distribution functions for the duration of the operating and repair states of the EV battery system are assumed to follow an exponential pattern. The hourly operational records for each EV battery system, including the system state and the duration spent in that state, can be determined using a process similar to the one utilized for a PV subsystem. Regarding the reliability of the EV battery system, the actual charging load Ld_{EV} for an EV is provided as:

$$Ld_{EV}(t)=Ld'_{EV}(t)\cdot S_{EV}(t) \tag{13}$$

where $Ld'_{EV}(t)$ is the charging demand of an EV at time t; and $S_{EV}(t)$ denotes the condition of the EV battery system at time t. If the system is operating, S_{EV} equals 1; otherwise, it equals 0.

C. EV Charging Strategy

The charging strategy for EVs includes coordinated and uncoordinated charging strategies. For each EV, the initial state of charge (SOC) of its battery is assumed to be uniformly distributed between 0.4 and 0.6, and the maximum SOC for the battery is set to be 80%.

For uncoordinated charging strategy, EVs with SOC under 40% will be charged immediately upon reaching the destination. For coordinated charging strategy, in order to utilize solar energy for charging EVs, the charging time for EVs with SOC under 40% is from 11:00 to 15:00. The flowchart for EV charging decisions is depicted in Fig. 3.

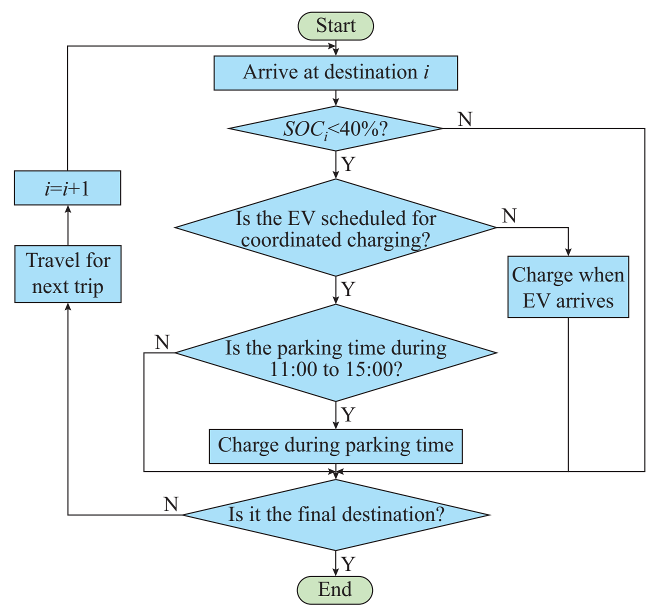

Fig. 3. Flowchart for EV charging decisions.

D. EV Load Demand Assessment for Different Sectors

This paper assumes that there are N EVs in the system and each EV user travels twice a day. The residential area is assumed to be the starting point of all EVs. Upon arrival at a location, the count of travel occurrences increases by one. The procedure for assessing EV load demands can be outlined as follows.

Step 1: the initial SOC, travel departure time, driving speed, and travel distance for the first travel of an EV are derived from probability density functions.

Step 2: based on the current location and the probabilities for the three functional areas, the travel destination is decided; and the travel distance for the next trip is determined based on probability density functions.

Step 3: upon reaching the destination, the travel time, arrival time, and battery SOC upon arrival are computed, and the parking duration at the destination is ascertained.

Step 4: determine the charging load demand at this destination according to the charging strategy and hourly operating history of the battery system within each EV.

Step 5: if an EV does not reach its final destination, go to *Step 2*.

Step 6: repeat *Steps 1-5* for all EVs.

Step 7: record the charging demands of each EV and determine the charging load demands for the three functional areas.

E. Adequacy Assessment of an Islanded System Embedded with PV and EVs

In a distribution system integrated with PV and EVs, annual load peak demand includes both the customer load peak demand and EV charging load peak demand. For different functional areas, the customer load demand and EV load demand are different. For a specific functional area, its RCR value RCR_{EV} can be calculated as:

$$RCR_{EV}=\frac{P_{PVnc}}{L_{cust}+L_{EV}} \tag{14}$$

where L_{EV} is the annual EV charging load peak demand in that area.

Considering EV load demands, LOLP is modified as:

$$LOLP=\frac{\sum_{t=1}^{8760N_Y} D'_t}{8760N_Y} \tag{15}$$

where D'_t equals 1 if $P_{pvsystem}$ is less than the sum of the EV load demand and customer load demand; otherwise, it equals 0.

PCENS is a metric utilized to assess the adequacy of EV charging, as represented in (16). It quantifies the proportion of EV load demand that the PV system cannot fulfill relative to the total EV load demand. A low PCENS value indicates that the PV islanded system can effectively meet the EV load demand.

$$PCENS=\frac{\sum_{i=1}^{N_Y}\sum_{j=1}^{N_{D_a}}\sum_{n=1}^{N} Ld_{EV,i}^{n}(D_a(j))}{\sum_{i=1}^{N_Y}\sum_{t=1}^{8760}\sum_{n=1}^{N} Ld_{EV,i}^{n}(t)} \tag{16}$$

where D_a is the time when D'_t equals 1; N_{D_a} is the total duration of the time when D'_t equals 1; N is the total number of EVs; $Ld_{EV,i}^{n}(D_a(j))$ is the charging load demand for EV n at time $D_a(j)$ in simulation year i; and $Ld_{EV,i}^{n}(t)$ is the charging load demand for EV n at time t in simulation year i.

An MCS method is utilized in this study to analyze the effect of different charging strategies on PV islanded system adequacy under different RCR_{EV}. The framework for the assessment is shown in Fig. 4, where T is the total simulation time; and $T_{\max}$ is the maximum time specified for the simulation.

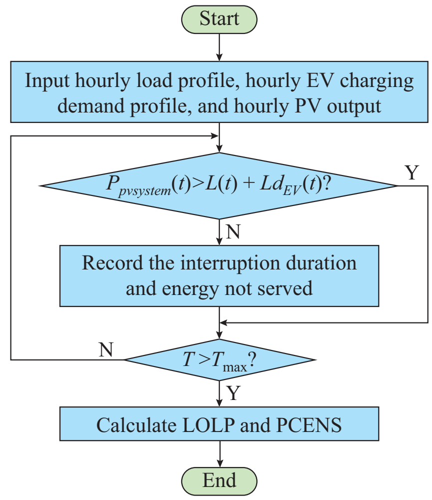

Fig. 4. Flowchart for PV islanded system adequacy assessment.

F. Assessment of EV Charging Service Reliability

In order to assess EV charging service reliability, AEVIFI and AEVIDI are defined and can be calculated using (17) and (18). AEVIFI represents the number of EV charging interruptions experienced per EV user within a given year, while AEVIDI denotes the duration of EV charging interruptions experienced per EV user within a year.

$$AEVIFI=\frac{\sum_{i=1}^{N_Y}\sum_{j=1}^{8760}\lambda_{ev,i}^{j}}{N_Y N} \tag{17}$$

$$AEVIDI=\frac{\sum_{i=1}^{N_Y}\sum_{j=1}^{8760}U_{ev,i}^{j}}{N_Y N} \tag{18}$$

where $\lambda_{ev,i}^{j}$ and $U_{ev,i}^{j}$ are the charging service interruption rate and annual average charging service interruption duration at hour j in simulation year i, respectively.

The flowchart for customer-side and EV-owner-side reliability assessments is shown in Fig. 5. The assumption in this study is that all system components, except for the lines and distribution transformers, function in a usual fashion. The TTF, TTR, and time to switch (TTS) for lines and distribution transformers follow an exponential distribution.

TTS can be determined as [22]:

$$TTS=-\frac{1}{\sigma}\ln R'' \tag{19}$$

where σ is the switching rate of the distribution system; and R'' denotes a sequence of random numbers that are uniformly distributed between 0 and 1.

IV. Case Study

In this section, the distribution system and the customer loads are introduced. In addition, simulations based on the test system are conducted to assess the PV islanded system adequacy and customer-side reliability for both the distribution system and EV charging service.

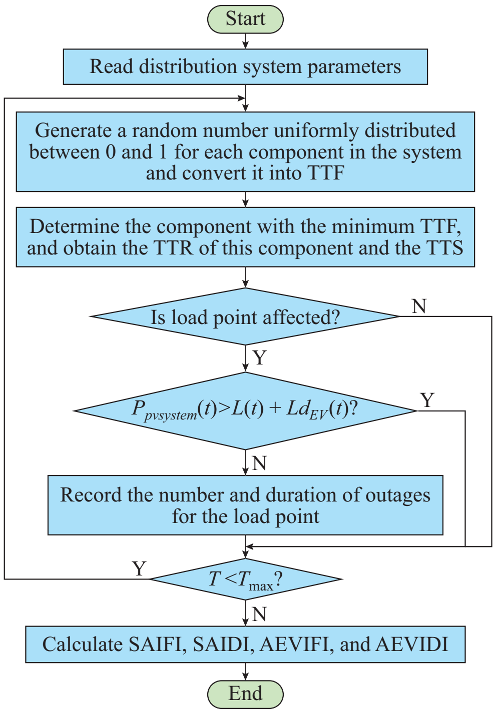

Fig. 5. Flowchart for customer-side and EV-owner-side reliability assessments.

A. System Description

This study utilizes a load duration curve to depict the variability in customer load for three distinct load demands [31]. The load model arranges the load data for each hour to simulate the hourly load behavior in the system, based on the hour of the day, the day of the week, and the week of the year. The development of a dynamic hourly load model $L(t)$ can be established as:

$$L(t)=L_y P_w P_d P_h(t) \tag{20}$$

where L_y is the annual peak load for each type of load demand; P_w is the proportion of the weekly load relative to the annual peak load; P_d is the proportion of the daily load relative to the weekly peak load; and $P_h(t)$ is the proportion of the hourly load relative to the daily peak load.

Due to the fact that loads are different in different areas, dividing customer loads into industrial, commercial, and residential loads is essential and the load demands are decided referencing load profiles in [32] and [33]. It is assumed that a consistent demand for charging load persists daily. Daily peak loads for different areas with uncoordinated EV load demand are shown in Fig. 6. Annual peak loads for industrial, residential, and commercial areas can be determined based on the daily peak loads in each specific area.

This paper employs a modified RBTS Bus 4 distribution system as a test system, as depicted in Fig. 7. In the case study, the adequacy assessment is conducted on the test system, which is supported by PV (i.e., PV islanded system), to assess the effect of PV systems on system reliability during interruptions. For the assessment of customer-side reliability, it is conducted on the test system supported by both PV and the main grid. The data regarding LPs and the reliability of system components can be referenced in [34]. In the test system, it is assumed that F1, F7, and F4 supply the industrial, commercial, and residential areas, respectively. In the three areas, PV system and EVs are connected at LP6 (industrial load), LP38 (commercial load), and LP25 (residential load).

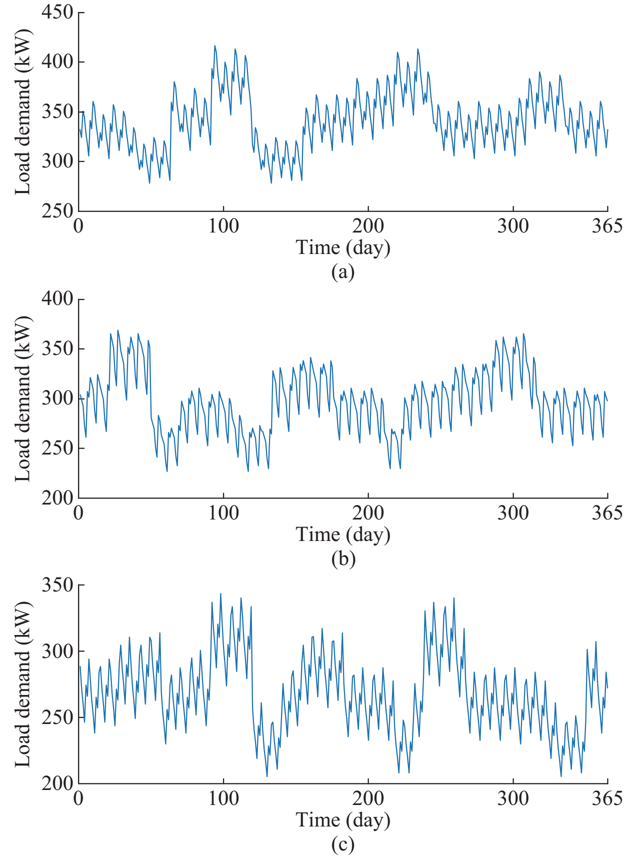

Fig. 6. Daily peak loads for different areas with uncoordinated EV load demand. (a) Industrial area. (b) Residential area. (c) Commercial area.

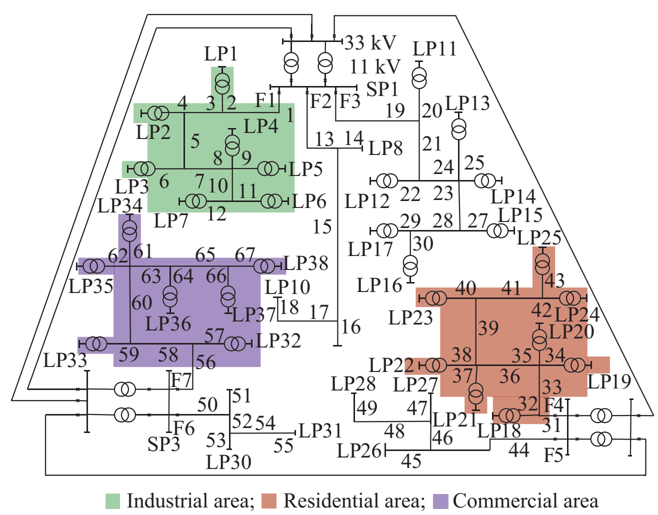

Fig. 7. Modified RBTS Bus 4 distribution system.

The historical solar radiation data used in this study to simulate the hourly output of the PV system over a year are obtained from the National Solar Radiation Database (NSRDB), USA, specifically from the Vichy Rolla National Airport station in Missouri [35]. It is assumed that there are

100 EVs in the urban area, and each EV user travels twice per day. The system parameters used in the simulation are shown in Table III, referring parameters in [36]. The reliability indices are assessed for various RCRs, charging strategies, and travel distances.

TABLE III
SYSTEM PARAMETERS

Parameter	Value
N	100
Initial SOC of EV battery	$U(0.4, 0.6)$
μ_0	6.92
σ_0	1.24
μ_l	10 km
σ_l	2.7 km
ω	70%
EV charging power	4 kW
The maximum SOC of EV battery	80%
λ_{sub}	0.381 failure per year
μ_{sub}	0.096 per hour
λ_{BEV}	8.361×10^{-6} failure per year
μ_{BEV}	0.081 per hour

B. Adequacy Assessment Simulation Outcomes

In this subsection, different scenarios are analyzed to study the impact of RCRs and EV load demands on the adequacy of the PV islanded system.

The LOLP values for different RCRs in the three areas without EVs are presented in Table IV. It can be observed that the increase of RCRs in all three areas results in a decrease in LOLP. This is attributed to the enhanced PV output facilitated by the rise in RCRs, thereby meeting the increased demand for load supply.

TABLE IV
LOLP VALUES FOR DIFFERENT RCRS IN THREE AREAS

Area	LOLP		
	$RCR=1$	$RCR=3$	$RCR=5$
Industrial	0.9474	0.7113	0.6516
Residential	0.7986	0.6487	0.6008
Commercial	0.9276	0.6860	0.6293

The impact of RCR_{EV} on the adequacy indices is studied under coordinated and uncoordinated charging strategies. Figure 8 shows the LOLP percentage changes in different areas based on the values in Table IV. It is demonstrated that for each RCR_{EV} value across the three areas, the LOLP values decrease in comparison to those outlined in Table IV because increasing PV system capacity leads to the increase of proportion of PV output over the load demands including the customer load and EV load demands. It is evident that the decrease in LOLP for each area is more pronounced under coordinated charging strategies compared with that under uncoordinated charging strategies. Under uncoordinated charging strategies, the charging period starts when EVs start charging at a particular time, whereas under coordinated charging strategies, the EV charging period is scheduled between 11:00 and 15:00, coinciding with the period with the optimal PV output. Consequently, the coordinated charging strategy allows for higher PV energy utilization, resulting in fewer hours for which the PV generation is lower than the load demand, and thus larger improvements in LOLP.

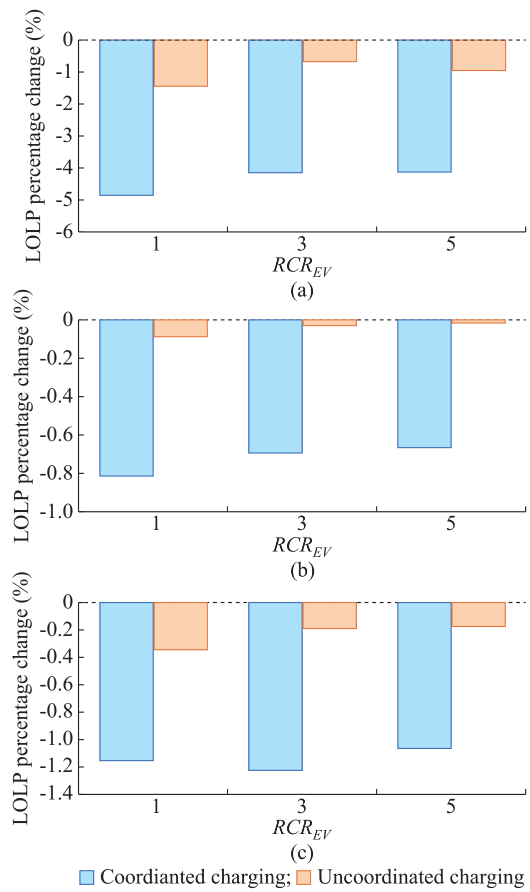

Fig. 8. LOLP percentage changes in different areas. (a) Industrial area. (b) Residential area. (c) Commercial area.

The PCENS values in different areas are shown in Fig. 9. Results show that PCENS decreases with an increase in RCR_{EV} for all areas, and PCENS values in each area are notably lower under coordinated charging strategies, primarily due to the increased utilization of PV energy. Under coordinated charging strategies, aligned with optimal PV output hours for charging EVs, the proportion of EV load demand that the PV system cannot fulfill relative to the total EV load demand is lower than that under uncoordinated charging strategies, resulting in the lower PCENS values.

C. Customer-side and EV Charging Service Reliability

To study the impact of travel distance on reliability, it is assumed that RCR_{EV} is 3 and the number of EVs is 100 in the simulation. SAIFI and SAIDI are used to evaluate the customer-side reliability of the distribution system for different EV travel distances.

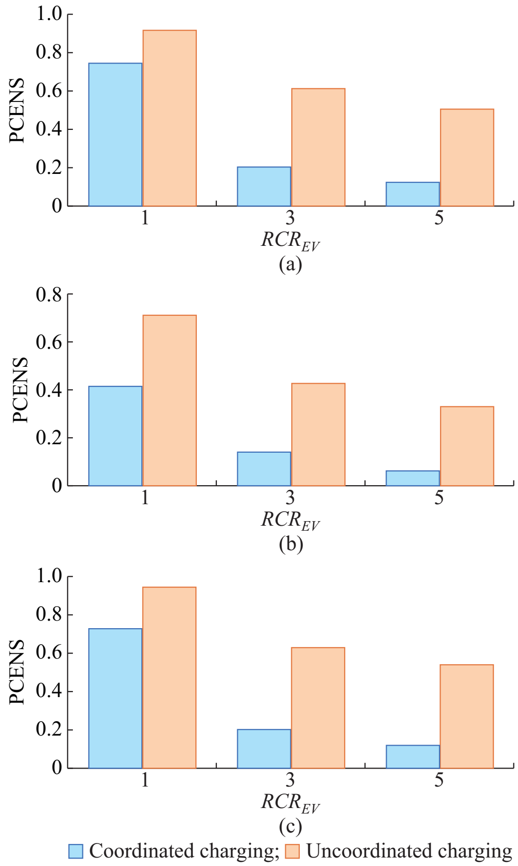

Fig. 9. PCENS values in different areas. (a) Industrial area. (b) Residential area. (c) Commercial area.

SAIFI represents the frequency of interruptions in the distribution system per customer within a year, while SAIDI represents the duration of interruptions in the distribution system per customer within a year. The values of SAIFI and SAIDI for the base case where the number of EVs is 0 are depicted in Table V. The two indices can be computed using (21) and (22).

TABLE V
VALUES OF SAIFI AND SAIDI

Area	SAIFI (failure per customer per year)	SAIDI (failure per customer per hour)
Industrial	0.7182	3.7565
Residential	0.6050	3.1728
Commercial	0.6422	3.3978

$$SAIFI=\frac{\sum_{i=1}^{N_Y}\sum_{j=1}^{N_{LP}}\lambda_i^j N_{cust,j}}{N_Y\sum_{j=1}^{N_{LP}}N_{cust,j}} \tag{21}$$

$$SAIDI=\frac{\sum_{i=1}^{N_Y}\sum_{j=1}^{N_{LP}}U_i^j N_{cust,j}}{N_Y\sum_{j=1}^{N_{LP}}N_{cust,j}} \tag{22}$$

where N_{LP} is the total number of LPs; $N_{cust,j}$ is the number of customers in LP j; and λ_i^j and U_i^j are the interruption rate and annual average interruption duration of LP j in simulation year i, respectively.

Figures 10-12 present the SAIFI and SAIDI percentage changes from the base case values in Table V under different average travel distances (μ_l) in the three different areas. The results reveal that in all areas, EV load demands for different travel distances lead to small changes of SAIFI and SAIDI of the system. This is due to that changes of EV load demands caused by different travel distances are relatively small compared with the customer loads in the distribution system. Results also indicate that coordinated charging improves the two indices in each area because of the higher utilization of PV energy.

Charging service reliability indices AEVIFI and AEVIDI are simulated for both coordinated and uncoordinated charging strategies, and the results are displayed in Figs. 13 and 14, respectively. It can be observed from Fig. 13 that for the industrial and commercial areas, as the travel distance increases, the values of AEVIFI and AEVIDI first decrease and then reach a certain value with small changes. This is because in the first trip, 70% EVs go to the industrial area and others go to the commercial area. Increasing the travel distance makes EVs arrive at the time when PV output can be used for charging purposes. For the residential area, the values first decrease and then fluctuate to a certain value. The first decrease is because as the travel distance increases, the PV output can be used at the arrival time of EVs in the residential area. But as the travel distance continues to increase, EVs arrive at a time when PV output decreases, therefore there is an increase in the two indices. Subsequently, under the coordinated charging strategy, the EV charging will be cutoff after 15:00, which is depicted by means of decrement in the indices when the travel distance increases over 35 km.

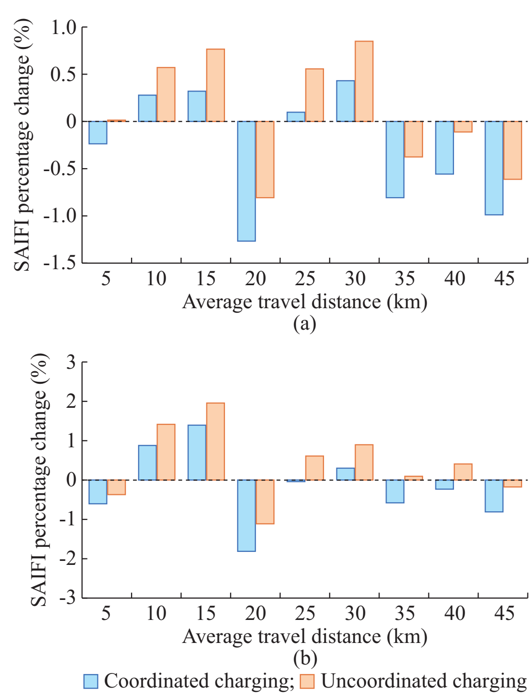

Fig. 10. SAIFI and SAIDI percentage changes in industrial area. (a) SAIFI percentage changes. (b) SAIDI percentage changes.

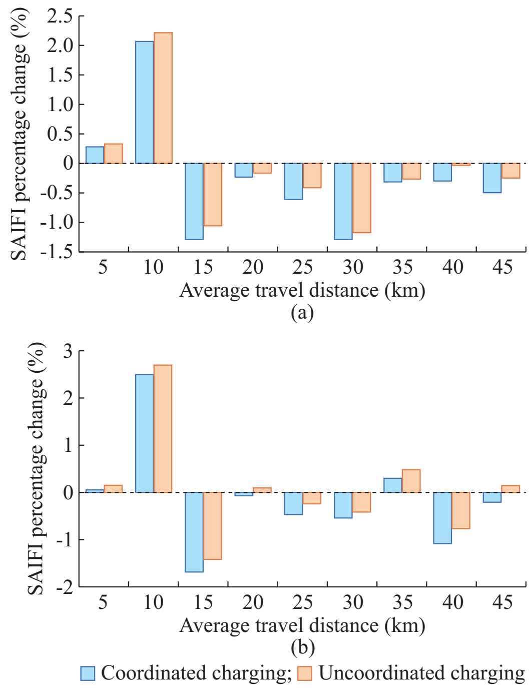

Fig. 11. SAIFI and SAIDI percentage changes in residential area. (a) SAIFI percentage changes. (b) SAIDI percentage changes.

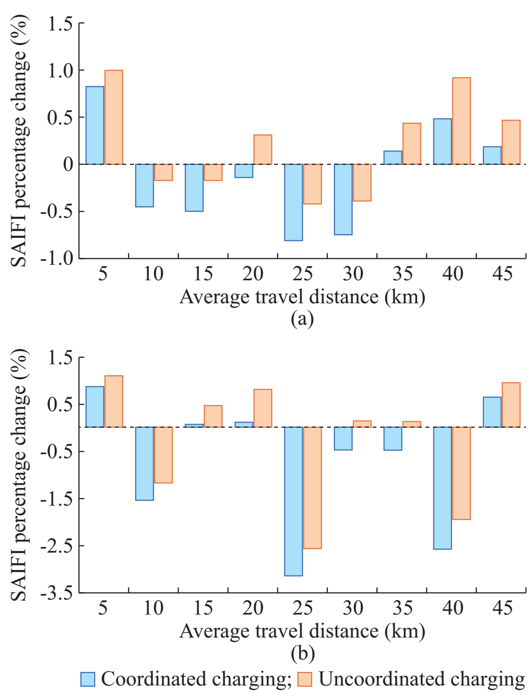

Fig. 12. SAIFI and SAIDI percentage changes in commercial area. (a) SAIFI percentage changes. (b) SAIDI percentage changes.

It can be observed from Fig. 14 that given the same travel distance, AEVIFI and AEVIDI under the coordinated charging strategy are much smaller than those under the uncoordinated charging strategy. When the travel distance is over 35 km, both AEVIFI and AEVIDI percentage changes have a great growth for the residential area. This is because, under the uncoordinated charging strategy, EVs arrive at the residential area at a time when no PV output can be used to charge. Hence, it can be concluded that AEVIFI and AEVIDI are improved significantly under the coordinated charging strategy.

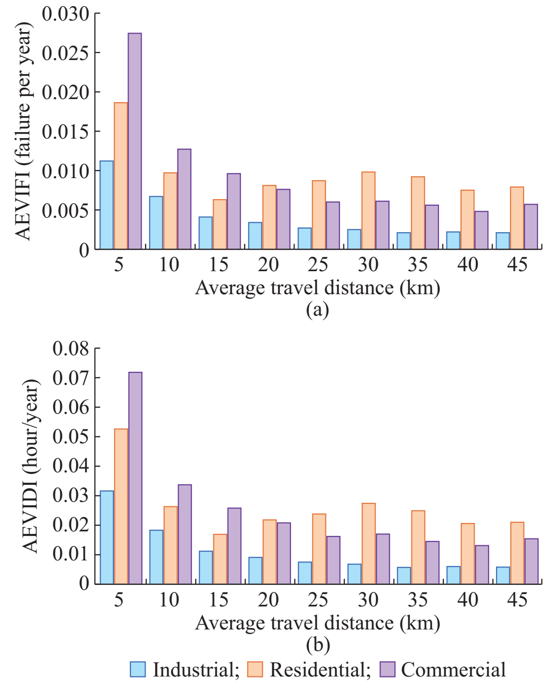

Fig. 13. AEVIFI and AEVIDI in different areas under coordinated charging strategies. (a) AEVIFI. (b) AEVIDI.

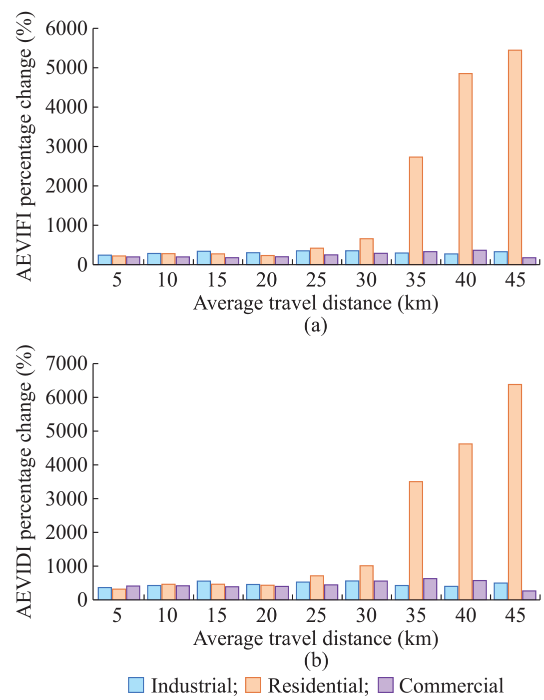

Fig. 14. AEVIFI and AEVIDI percentage changes in different areas under uncoordinated charging strategies. (a) AEVIFI percentage changes. (b) AEVIDI percentage changes.

D. Comparative Analysis of AEVIFI and AEVIDI for Different Areas

In this subsection, an additional scenario to illustrate the effects of altering area distributions on simulation outcomes is introduced. In case 1, the residential and commercial areas are swapped, and the reliability indices between the original configuration (base case) and case 1 are compared. The indices for these configurations are depicted in Tables VI-IX.

TABLE VI
AEVIFI FOR BASE CASE

Area	Charging strategy	AEVIFI (failure per year)					
		5 km	10 km	15 km	20 km	25 km	30 km
Industrial	Uncoordinated	0.0377	0.0202	0.0177	0.0141	0.0121	0.0115
	Coordinated	0.0112	0.0053	0.0041	0.0033	0.0028	0.0026
Residential	Uncoordinated	0.0586	0.0343	0.0259	0.0279	0.0384	0.0863
	Coordinated	0.0173	0.009	0.0073	0.0083	0.0093	0.0088
Commercial	Uncoordinated	0.0808	0.0335	0.0241	0.0226	0.0238	0.0197
	Coordinated	0.0253	0.0119	0.0081	0.0075	0.0070	0.0051

TABLE VII
AEVIFI FOR CASE 1

Area	Charging strategy	AEVIFI (failure per year)					
		5 km	10 km	15 km	20 km	25 km	30 km
Industrial	Uncoordinated	0.0405	0.0219	0.0185	0.0140	0.0124	0.0120
	Coordinated	0.0116	0.0061	0.0040	0.0033	0.0026	0.0022
Residential	Uncoordinated	0.0584	0.0351	0.0254	0.0281	0.0409	0.0905
	Coordinated	0.0195	0.0100	0.0079	0.0082	0.0105	0.0103
Commercial	Uncoordinated	0.0699	0.0346	0.0225	0.0204	0.0217	0.0211
	Coordinated	0.0215	0.0103	0.0077	0.0067	0.0063	0.0053

TABLE VIII
AEVIDI FOR BASE CASE

Area	Charging strategy	AEVIDI (hour/year)					
		5 km	10 km	15 km	20 km	25 km	30 km
Industrial	Uncoordinated	0.1418	0.0726	0.0672	0.0534	0.0455	0.0466
	Coordinated	0.0305	0.0142	0.0113	0.0090	0.0079	0.0070
Residential	Uncoordinated	0.2132	0.1265	0.1067	0.1135	0.1604	0.3513
	Coordinated	0.0484	0.0240	0.0202	0.0222	0.0255	0.0231
Commercial	Uncoordinated	0.3380	0.1375	0.1001	0.1022	0.1086	0.0817
	Coordinated	0.0601	0.0329	0.0224	0.0216	0.0183	0.0142

TABLE IX
AEVIDI FOR CASE 1

Area	Charging strategy	AEVIDI (hour/year)					
		5 km	10 km	15 km	20 km	25 km	30 km
Industrial	Uncoordinated	0.1406	0.0769	0.0739	0.0525	0.0502	0.0399
	Coordinated	0.0310	0.0165	0.0111	0.0085	0.0073	0.0061
Residential	Uncoordinated	0.2157	0.1337	0.1019	0.1142	0.1810	0.4070
	Coordinated	0.0531	0.0268	0.0225	0.0222	0.0289	0.0262
Commercial	Uncoordinated	0.2911	0.1396	0.0971	0.0891	0.0959	0.0893
	Coordinated	0.0584	0.0280	0.0210	0.0187	0.0170	0.0146

The data indicate that exchanging residential and commercial areas has minimal impact on the indices. It is noted that exchanging any two areas within the test system results in similar outcomes, suggesting a minimal impact of altering the distribution system structure on the reliability of EV charging services.

V. CONCLUSION

This paper introduces an MCS-based approach for assessing the effects of spatial-temporal distribution of charging demand by EVs and PV output on the adequacy and customer-side reliability indices for both the distribution system and EV charging services. To improve the accuracy of evaluating reliability in both the distribution system and charging service, multi-state and two-state models for the PV system and EV battery system, respectively, are developed to incorporate the failure rates of components within these systems.

Furthermore, the impact of cloud movements on energy outputs of the PV system is also taken into account. New indices are defined to analyze both the adequacy of EV charging services and reliability from the perspective of EV owners.

The associated results are evaluated to showcase the impacts of different RCR values of the PV system and the movement of EVs under different charging strategies on the distribution system and charging service reliability. This work can be utilized to provide insights into enhancing the reliability of charging services across diverse functional areas with differing customer loads within a distribution system. The proposed approach is implemented on a modified RBTS Bus 4 distribution system, and the simulation results show the reliability indices for the EV charging service such as PCENS, AEVIFI, and AEVIDI are improved under the coordinated charging strategy. Furthermore, travel distances have an influence on the reliability indices of the charging service, as they influence the arrival time of EVs. When EVs are charged during periods of surplus PV energy availability, the system reliability is enhanced. Exchanging any two areas within the test system does have minimal impact on the reliability of EV charging services.

References

[1] T. Qian, C. Shao, X. Li *et al*., "Enhanced coordinated operations of electric power and transportation networks via EV charging services," *IEEE Transactions on Smart Grid*, vol. 11, no. 4, pp. 3019-3030, Jan. 2020.

[2] K. Clement-Nyns, E. Haesen, and J. Driesen, "The impact of charging plug-in hybrid electric vehicles on a residential distribution grid," *IEEE Transactions on Power Systems*, vol. 25, no. 1, pp. 371-380, Feb. 2010.

[3] A. Ovalle, J. Fernandez, A. Hably *et al*., "An electric vehicle load management application of the mixed strategist dynamics and the maximum entropy principle," *IEEE Transactions on Industrial Electronics*, vol. 63, no. 5, pp. 3060-3071, May 2016.

[4] K. Lappalainen and S. Valkealahti, "Output power variation of different PV array configurations during irradiance transitions caused by moving clouds," *Applied Energy*, vol. 190, pp. 902-910, Mar. 2017.

[5] D. Dallinger and M. Wietschel, "Grid integration of intermittent renewable energy sources using price-responsive plug-in electric vehicles," *Renewable and Sustainable Energy Reviews*, vol. 16, no. 5, pp. 3370-3382, Jun. 2012.

[6] T. Adefarati and R. C. Bansal, "Reliability assessment of distribution system with the integration of renewable distributed generation," *Applied Energy*, vol. 185, pp. 158-171, Jan. 2017.

[7] I. S. Bae and J. O. Kim, "Reliability evaluation of customers in a microgrid," *IEEE Transactions on Power Systems*, vol. 23, no. 3, pp. 1416-1422, Aug. 2008.

[8] M. Al-Muhaini and G. T. Heydt, "Evaluating future power distribution system reliability including distributed generation," *IEEE Transactions on Power Delivery*, vol. 28, no. 4, pp. 2264-2272, Oct. 2013.

[9] P. M. de Quevedo, J. Contreras, A. Mazza *et al*., "Reliability assessment of microgrids with local and mobile generation, time-dependent profiles, and intraday reconfiguration," *IEEE Transactions on Industry Applications*, vol. 54, no. 1, pp. 61-72, Jan. 2018.

[10] W. Zhong, L. Wang, Z. Liu *et al*., "Reliability evaluation and improvement of islanded microgrid considering operation failures of power electronic equipment," *Journal of Modern Power Systems and Clean Energy*, vol. 8, no. 1, pp. 111-123, Mar. 2020.

[11] S. Conti, R. Nicolosi, and S. A. Rizzo, "Generalized systematic approach to assess distribution system reliability with renewable distributed generators and microgrids," *IEEE Transactions on Power Delivery*, vol. 27, no. 1, pp. 261-270, Jan. 2012.

[12] B. Zeng, Y. Luo, C. Zhang *et al*., "Assessing the impact of an EV battery swapping station on the reliability of distribution systems," *Applied Sciences*, vol. 10, no. 22, p. 8023, Nov. 2020.

[13] L. Xiao, K. M. Muttaqi, and A. P. Agalgaonkar, "Reliability assessment of modern distribution networks embedded with renewable and distributed resources," *Electric Power Systems Research*, vol. 212, p. 108374, Nov. 2022.

[14] L. Cheng, Y. Chang, J. Lin *et al*., "Power system reliability assessment with electric vehicle integration using battery exchange mode," *IEEE Transactions on Sustainable Energy*, vol. 4, no. 4, pp. 1034-1042, Oct. 2013.

[15] G. Li, Z. Bie, H. Xie *et al*., "Customer satisfaction based reliability evaluation of active distribution networks," *Applied Energy*, vol. 162, pp. 1571-1578, Jan. 2016.

[16] T. Fan, Y. Liu, S. Du *et al*., "Reliability evaluation based on Monte Carlo simulation considering islanded operation in distribution network with microgrid," in *Proceedings of International Conference on Renewable Power Generation*, Beijing, China, Oct. 2015, pp. 1-7.

[17] H. Farzin, M. Moeini-Aghtaie, and M. Fotuhi-Firuzabad, "Reliability studies of distribution systems integrated with electric vehicles under battery-exchange mode," *IEEE Transactions on Power Delivery*, vol. 31, no. 6, pp. 2473-2482, Dec. 2016.

[18] H. Farzin, M. Fotuhi-Firuzabad, and M. Moeini-Aghtaie, "Reliability studies of modern distribution systems integrated with renewable generation and parking lots," *IEEE Transactions on Sustainable Energy*, vol. 8, no. 1, pp. 431-440, Jan. 2017.

[19] P. Xue, Y. Xiang, J. Gou *et al*., "Impact of large-scale mobile electric vehicle charging in smart grids: a reliability perspective," *Frontiers in Energy Research*, vol. 9, p. 688034, Jun. 2021.

[20] T. M. Aljohani and M. J. Beshir, "MATLAB code to assess the reliability of the smart power distribution system using Monte Carlo simulation," *Journal of Power and Energy Engineering*, vol. 5, no. 8, pp. 30-44, Aug. 2017.

[21] Z. Bie, P. Zhang, G. Li *et al*., "Reliability evaluation of active distribution systems including microgrids," *IEEE Transactions on Power Systems*, vol. 27, no. 4, pp. 2342-2350, Nov. 2012.

[22] R. Billinton and W. Li, *Reliability Assessment of Electric Power Systems Using Monte Carlo Methods*. Boston: Springer Science & Business Media, 1994.

[23] A. A. Chowdhury and D. O. Koval, *Power Distribution System Reliability*. Hoboken: John Wiley & Sons, 2011.

[24] L. Xiao, K. M. Muttaqi, and A. P. Agalgaonkar, "Improving reliability of PV-powered highway with electric vehicle charging services," *IEEE Transactions on Industry Applications*, vol. 60, no. 2, pp. 2002-2011, Mar. 2024.

[25] K. G. T. Hollands and R. G. Huget, "A probability density function for the clearness index, with applications," *Solar Energy*, vol. 30, no. 3, pp. 195-209, Nov. 1983.

[26] Z. Liu, F. Wen, and G. Ledwich, "Optimal siting and sizing of distributed generators in distribution systems considering uncertainties," *IEEE Transactions on Power Delivery*, vol. 26, no. 4, pp. 2541-2551, Oct. 2011.

[27] P. Zhang, Y. Wang, W. Xiao *et al*., "Reliability evaluation of grid-connected photovoltaic power systems," *IEEE Transactions on Sustainable Energy*, vol. 3, no. 3, pp. 379-389, Jul. 2012.

[28] L. Zhang, K. Sun, Y. Xing *et al*., "A modular grid-connected photovoltaic generation system based on DC bus," *IEEE Transactions on Power Electronics*, vol. 26, no. 2, pp. 523-531, Feb. 2011.

[29] T. Yi, C. Zhang, T. Lin *et al*., "Research on the spatial-temporal distribution of electric vehicle charging load demand: a case study in China," *Journal of Cleaner Production*, vol. 242, p. 118457, Jan. 2020.

[30] X. Shu, W. Yang, Y. Guo *et al*., "A reliability study of electric vehicle battery from the perspective of power supply system," *Journal of Power Sources*, vol. 451, p. 227805, Mar. 2020.

[31] P. Wang and R. Billinton, "Time sequential distribution system reliability worth analysis considering time varying load and cost models," *IEEE Transactions on Power Delivery*, vol. 14, no. 3, pp. 1046-1051, Jul. 1999.

[32] S.-A. Yin and C.-N. Lu, "Distribution feeder scheduling considering variable load profile and outage costs," *IEEE Transactions on Power Systems*, vol. 24, no. 2, pp. 652-660, May 2009.

[33] K. Qian, C. Zhou, M. Allan *et al*., "Modeling of load demand due to EV battery charging in distribution systems," *IEEE Transactions on Power Systems*, vol. 26, no. 2, pp. 802-810, May 2011.

[34] R. N. Allan, R. Billinton, I. Sjarief *et al*., "A reliability test system for

educational purposes-basic distribution system data and results," *IEEE Transactions on Power Systems*, vol. 6, no. 2, pp. 813-820, May 1991.

[35] National Centers for Environmental Information. (2024, Jan.). National solar radiation database. [Online]. Available: https://www. ncei. noaa. gov/products/land-based-station/national-solar-radiation-database

[36] A. K. Karngala and C. Singh, "Reliability assessment framework for the distribution system including distributed energy resources," *IEEE Transactions on Sustainable Energy*, vol. 12, no. 3, pp. 1539-1548, Jan. 2021.

Lei Xiao received the B. S. degree from Central South University, Changsha, China, in 2009, and the M. S. degree from Arizona State University, Tempe, USA, in 2015. She is currently pursuing the Ph.D. degree in University of Wollongong, Wollongong, Australia. Her research interests include power system reliability and resilience, renewable energy, and distributed generation.

Kashem M. Muttaqi received the B.Sc. degree from Bangladesh University of Engineering and Technology (BUET), Dhaka, Bangladesh, in 1993, the M.Eng.Sc. degree from University of Malaya, Kuala Lumpur, Malaysia, in 1996, and the Ph. D. degree from Multimedia University, Selangor, Malaysia, in 2001. He is the Director of the ARC Training Centre in Energy Technologies for Future Grids, sponsored by Australian Government, and several industries and universities in Australia. He is a Senior Professor and the Discipline Leader - Electrical Engineering at the School of Electrical, Computer and Telecommunications Engineering, University of Wollongong, Wollongong, Australia. He was associated with the University of Tasmania, Hobart, Australia, as a Research Fellow/Lecturer/Senior Lecturer from 2002 to 2007, and with the Queensland University of Technology, Brisbane, Australia, as a Research Fellow from 2000 to 2002. Previously, he worked for Multimedia University as a Lecturer for three years. He is a Fellow of the Institution of Engineers Australia (FIEAust), a Fellow of the Institution of Engineering and Technology UK (FIET), and a Fellow of the Institute of Electrical and Electronics Engineers (IEEE). His research interests include electric vehicle, energy technology, distributed generation, solid state transformer, power converter, power electronics application, renewable energy, solar PV, wind turbine, wave energy, smart grid, micro-grid, standalone power supply, and power system planning and control.

Ashish P. Agalgaonkar received the Ph.D. degree from the Indian Institute of Technology Bombay, Mumbai, India, in 2006. He was a Scientist at the Energy Technology Centre, NTPC Ltd., Greater Noida, India, from 2005 to 2007, and was associated with the University of Tasmania, Hobart, Australia, as a Postdoctoral Research Fellow from October 2007 to January 2008. In February 2008, he took up a position at the University of Wollongong, Wollongong, Australia, as a Postdoctoral Research Fellow. He was a Postdoctoral Research Fellow until November 2010 before taking up a Lecturer position at the University of Wollongong in December 2010. He is currently an Associate Professor at the University of Wollongong. His research interests include planning and operational aspects of renewable and distributed generation, power system reliability, microgrid, electricity market, and system stability.